

See discussions, stats, and author profiles for this publication at: <https://www.researchgate.net/publication/231637222>

Theoretical Investigation of Small Alkali Cation –Molecule Clusters: A Model Potential Approach

ARTICLE in THE JOURNAL OF PHYSICAL CHEMISTRY B · DECEMBER 2003

Impact Factor: 3.3 · DOI: 10.1021/jp036075h

CITATIONS

9

READS

5

7 AUTHORS, INCLUDING:



Christine Cézard

Université de Picardie Jules Verne

16 PUBLICATIONS 204 CITATIONS

SEE PROFILE



Benjamin Bouvier

Institute for the Biology and Chemistry of Pro...

17 PUBLICATIONS 379 CITATIONS

SEE PROFILE



Jean-Pierre Dognon

Atomic Energy and Alternative Energies Com...

75 PUBLICATIONS 1,325 CITATIONS

SEE PROFILE

Theoretical Investigation of Small Alkali Cation–Molecule Clusters: A Model Potential Approach

C. Cézard,[†] B. Bouvier,[†] V. Brenner,[†] M. Defranceschi,[‡] Ph. Millié,[§] J. M. Soudan,[†] and J. P. Dognon^{*,†}

CEA/Saclay, DSM/DRECAM/SPAM-LFP (CEA-CNRS URA2453), Bat. 522, 91191 Gif sur Yvette, France, CEA Saclay, DEN/DSOE/RB, and Paris-Sud University, Bat. 350, 91405 Orsay Cedex, France

Received: July 17, 2003; In Final Form: October 28, 2003

We present here a model potential study of the microsolvation of alkali cations M^+ ($M = \text{Na}, \text{K}, \text{Rb}, \text{Cs}$) in various solvents (water, methanol, dimethyl ether (DME)). The potential energy surfaces (PES) are explored with the Monte Carlo growth method (MCGM) to find the most significant equilibrium structures of $M^+(\text{solvent})_n$ clusters ($n = 2, 4$). The structures as well as the binding energies are favorably compared to the best ab initio calculations found in the literature and to experimental results. This good agreement is only obtained if we take into account the anisotropy of the polarizability tensor for the solvent molecule. Under these conditions, the atomic parameters included in our model potential framework are found to be transferable from water to methanol and DME. An analysis of the different physical components of the interaction energy shows that the only important n -body term for the description of these systems is the polarization one.

1. Introduction

Systems consisting of an alkali metal cation (M^+) and one or more neutral ligands (L) are involved in many processes. Noncovalent metal–ligand interactions play a primary role in many biological processes (for example, discrimination of Na^+ vs K^+), or in nuclear fuel reprocessing, where solvent extraction is used to remove alkali cations from radioactive nuclear waste. In this last case, crown-ether ligands are known to bind selectively to a given alkali metal cation. This selectivity is found to be influenced by the nature of the solvent.^{1–3} Indeed, in fuel reprocessing solutions, both the cations and crown complexes are surrounded by molecules of solvent. Therefore, the cation/crown complexation is the result of the competition between the different interactions that govern such systems (i.e., cation–solvent, cation–crown, solvent–solvent, solvent–crown, etc.).

A first step toward a quantitative analysis of these competition phenomena is to perform a theoretical study of the microsolvation of alkali cations M^+ ($M = \text{Na}, \text{K}, \text{Rb}, \text{Cs}$) by various solvents, to gain a better understanding of the interactions of ions with their local environment, and notably to evaluate the role of some atomic (cations) and/or molecular (solvent) properties on the structure of the solvation shells. In this way, we will pay attention to the influence of the dipole moment of the solvents, of the electric dipole polarizability of both cations and solvents, of the hydrogen bonds between two molecules of solvent and of possible steric hindrance effects. For this purpose, we have chosen a cluster approach. Water, methanol, and dimethyl ether (DME) were chosen as solvent molecules. From a theoretical point of view, the interest of such a choice lies in the gradual change of their permanent dipole moment and their electric dipole polarizability, the first decreasing and the second

increasing along the series. In addition, DME, unlike water and methanol, does not form hydrogen bonds. Moreover, the M^+ –DME system is a good model for the study of the cation/crown ether interaction. From a more practical point of view, methanol is used in a wide variety of chemical processes and more precisely, water–methanol mixture is employed as solvent in numerous experimental measurements.

So far, studies of ion–solvent complexes are very often limited to water as the solvent, and in this context, many theoretical and experimental publications exist. It appears virtually impossible to acknowledge the large amount of literature on this topic, and throughout this article only a few selected references that are important for the present work are given. Conversely, unlike water, the literature is quite sparse on the clustering of alkali cations with methanol or DME molecules.

Numerous theoretical investigations, by means of ab initio calculations, already exist in the field of alkali cation microsolvation, at various levels of theory and with different basis sets.^{4–9} We decided not to use an ab initio method, but rather a model potential one. The reasons for such a choice are the following:

(i) One can study larger systems and obtain their associated binding energy more easily. In particular, the basis set superposition error (BSSE) correction, which is a very time-consuming procedure in ab initio calculations of large clusters, is suppressed.

(ii) One can extensively explore the corresponding potential energy surface (PES) by means of global optimization methods, without any constraints on the starting structures.

(iii) It is possible to obtain, in clusters with several molecules, the different physical components of the total interaction energy separately, providing the finest description of the competition phenomena.

(iv) One can obtain an accurate model potential for molecular dynamics simulation to properly take into account entropic effects and/or describe time dependent phenomena.

* Corresponding author. E-mail: jean-pierre.dognon@cea.fr.

[†] CEA/Saclay, DSM/DRECAM/SPAM-LFP (CEA-CNRS URA2453).

[‡] CEA Saclay, DEN/DSOE/RB.

[§] Paris-Sud University.

From this last point of view, it is interesting to recall that the number of solvent molecules in the first solvation sphere may differ in a cluster and in the liquid phase. For example, the sodium cation is surrounded by six water molecules in the liquid phase and by four in clusters.^{10,11}

As we want to study the solvation of the series of the alkali cations into different solvents, the model potential we will use must possess some important features:

(i) As the cations and the solvents show an important variation of their polarizability (it increases from Na⁺ to Cs⁺ and from water to dimethyl ether), the polarization energy must be accurately calculated to properly take into account these variations.

(ii) To describe the structure of the different solvation shells, the hydrogen bonds have to be well described.

(iii) As far as possible, some atomic parameters of the intermolecular model potential have to be transferable both for the alkali cations and for some atoms of the solvent molecules in chemically equivalent situations.

The model potential, used by Derepas et al.¹² in a previous work to study the hydration of Na⁺ and Cs⁺, integrates many of the aforementioned properties. We will use the same model potential framework and the same building strategy: in these potentials only two atomic parameters are introduced to describe the short-range interactions. Therefore, our goals throughout this study are manifold:

(i) Complete the series of the M⁺–H₂O model potentials for K⁺ and Rb⁺ cations (the Na⁺–H₂O, Cs⁺–H₂O, and H₂O–H₂O model potential have been already established in ref 12).

(ii) Test the transferability of the two atomic parameters for the alkali cations and the oxygen atom from one system to another.

(iii) Test the reliability of our model potentials by comparing our results on small clusters M⁺–L_n (*n* = 2–4) with already published ab initio and/or experimental ones.

The outline of this paper is as follows. The first section describes the model potential framework, the strategy, and the methodology we use to build it, as well as the way we explore the potential energy surfaces. The second section deals with the M⁺–(H₂O) systems, the establishment of their model potentials and the transferability of their atomic parameters to the other systems. Finally, the third section discusses the geometries and the binding energies of the clusters we obtained with all the cations and up to four molecules of solvent; a systematic comparison with previous results of the literature will be made.

2. Methodology

2.1. Model Potential. We have used the same model potential framework designed for the treatment of intermolecular interactions as the one of Derepas et al.¹² Because the strategy has already been described in detail,¹² we only report here the main features and the enhancements we have added.

The geometries of the molecules are kept frozen and the interaction energy E_{int} is expressed as follows:

$$E_{\text{int}} = E_{\text{elec}} + E_{\text{pol}} + E_{\text{disp}} + E_{\text{rep}} + E_{\text{disp-exch}}$$

All these contributions to the interaction energy, namely electrostatic, polarization, dispersion, repulsion, and dispersion-exchange components are expressed by analytical formulas, derived from a second-order exchange perturbation treatment.

An important feature of the model potential we use is that the formulas used to describe the electrostatic and polarization

terms ensure accuracy at long distances, equivalent to that obtained with reliable ab initio calculations. The electrostatic contribution E_{elec} , which is the only two-body term in the previous expression, is described via interacting multipolar multicentric distributions on each monomer and these distributions are derived from an ab initio calculation. The electric field created by the permanent molecular multipoles is calculated using the same multipolar expansion. The *n*-body character of the polarization term (E_{pol}) is taken into account and includes the back-polarization contribution and the induced dipole–induced dipole interaction. To describe the anisotropy of the molecular electric dipole polarizabilities (in ref 12, only the scalar average molecular polarizability is used), we start from the theory of Lefevre et al.¹³ According to this, the scalar molecular polarizabilities ($\bar{\alpha}_{\text{M}}$) are obtained from average *kl* bond polarizabilities ($\bar{\alpha}_{kl}$) by using an additive rule,

$$\bar{\alpha}_{\text{M}} = \sum_{kl} \bar{\alpha}_{kl}$$

(such an additive rule is experimentally well checked in our systems). Each *kl* bond polarizability is described via transversal (T) and longitudinal (L) components so that $\bar{\alpha}_{kl} = 1/3(\alpha_{kl}^{\text{L}} + 2\alpha_{kl}^{\text{T}})$ and we adjust the ratio $\alpha_{kl}^{\text{L}}/\alpha_{kl}^{\text{T}}$ ($\bar{\alpha}_{kl}$ is kept unchanged) to reproduce the experimental molecular anisotropy when available, otherwise the ab initio one (see the appendix for more details).

The repulsion (E_{rep}) and dispersion (E_{disp}) expressions are described by sums of atom–atom terms, in which atom-dependent parameters are introduced. The analytical formulas used to express the above contributions are derived from Kitaigorodskii's:¹⁴

$$E_{\text{rep}} + E_{\text{disp}} + E_{\text{disp-exch}} = \sum_i \sum_j k_i k_j \left[G_{ij} C \exp(-\gamma z) - \left(\frac{C_6}{z^6} + \frac{C_8}{z^8} + \frac{C_{10}}{z^{10}} \right) + G_{ij} C^{\text{de}} \exp(-\gamma^{\text{de}} z) \right]$$

where

$$z = r_{ij}/r_{ij}^0 \quad r_{ij}^0 = \sqrt{(2R_i^{\text{w}})(2R_j^{\text{w}})}$$

$$G_{ij} = (1 - Q_i/n_i^{\text{val}})(1 - Q_j/n_j^{\text{val}})$$

Two kinds of parameters are used in these formulas: “standard” ones (C_6 , C_8 , C_{10} , C , γ , C^{de} , γ^{de}), not atom-dependent and “atomic” ones (i.e., atom-dependent). The atom-dependent parameters contained in these equations are k_i and R_i^{w} . In the initial treatment, R_i^{w} is approximated as the van der Waals radii of atoms. A more detailed discussion of the parameter's physical signification could be found in refs 15 and 16.

As the electrostatic and polarization components (of the interaction energy) are, with a very good accuracy, equivalent to the ab initio ones, this allows us to obtain the repulsion and dispersion terms by fitting the model potential interaction energy onto the ab initio one. Of course, for this purpose, we use *at this stage* the ab initio polarizability components. The O and H parameters were derived from ab initio calculations on the water dimer.¹² In all the following, they are assumed fixed and transferable. The corresponding atom-dependent parameters for the alkali cation are extracted from ab initio MP2 calculations performed on the M⁺–one water molecule system. At this stage, it should be pointed out that reliable ab initio calculations take into account more short-range effects than the exchange-

repulsion one, such as attractive charge transfer, repulsive exchange-polarization, penetration effects, etc. These effects are then implicitly included in the model potential short-range term.

2.2. Potential Energy Surfaces (PES) Exploration Method.

The PES exploration method used in this study is the Monte Carlo growth method (MCGM). It was first developed by Garel and al.^{15,16} for the study of macromolecules. Then it has been successfully applied to metal clusters,^{17,18} to homogeneous clusters,¹⁹ and finally to heterogeneous clusters.^{12,20} We will not describe in detail the method here, as this has been done in the previously cited references. Briefly, the MCGM consists of growing the clusters molecule per molecule (in our case the molecule can be either the alkali cation or a solvent molecule), to generate a Boltzmann sample of configurations for each cluster size at a fictitious temperature T . These configurations are then locally optimized by the pseudo Newton method (BFGS),^{21–23} and the Hessian is calculated to confirm that true minima are obtained.

Many growths at different temperatures (175–600 K) were performed for an extensive exploration of the potential energy surface. We have also used different strategies of growth, varying the position of insertion of the cation in the growing process. For example, if the cation is the last inserted particle, “surface” structures are favored.

2.3. Computational Details. To first obtain the K^+ and Rb^+ atomic parameters for the model potential, and then to verify the transferability of the parameters of all the alkali cations to systems involving another solvent, we have to perform reliable ab initio calculations. Moreover, the same basis sets and the same theoretical method have to be used to calculate both the multipolar multicentric distribution of each solvent molecule and the ab initio interaction energy in the cation–molecule system. For this purpose, we have chosen the MP2 method, which leads to very good results for analogous systems (see for example ref 24). Additionally, some relevant properties have to be well reproduced: for the cations, the electric dipole polarizability and the first ionization potential; for each solvent molecule, the first nonzero multipole moment, the molecular polarizability and the vertical ionization potential. Thus, the basis sets should be judiciously chosen. For oxygen, carbon, and hydrogen, the basis sets are built from van Duijneveldt ones²⁴ and are equivalent to quadruple- ζ valence basis sets plus polarization functions (two d functions, whose exponents are (1.5 and 0.35) and (1.335 and 0.288) were added for oxygen and carbon, respectively, and two p functions (1.4 and 0.25) for hydrogen). All the alkali cations are described by a small-core average relativistic effective core potential (AREP). The AREPs of Christiansen et al. have been used for Na^+ ,²⁵ K^+ ,²⁶ Rb^+ ,²⁷ and Cs^+ .²⁸ Therefore, for all the cations, eight electrons (ns^2np^6 configuration) are explicitly taken into account. For Na^+ , the original basis set (6s4p) associated with this AREP was contracted and increased to obtain a (4s4p3d) basis set.²⁰ For K^+ , Rb^+ , and Cs^+ the AREP's consist of a core of respectively 10, 28, and 46 electrons. For the associated basis sets of these three alkali cations, we started from Hoyau et al.'s ones,²⁹ and we included additional polarization and diffuse functions to better reproduce the properties of the cations, especially the first ionization potential (the corresponding basis sets can be obtained upon request). The frozen geometry of each solvent molecule is the most stable one at the MP2 level.

Unless otherwise specified, all M^+L ab initio binding energies computed in this work were basis set superposition error (BSSE) corrected using the counterpoise correction of Boys and Bernardi.³⁰

TABLE 1: Polarizability and Ionization Potential (IP) of the Cations Both from Experiments and ab Initio MP2 Calculations

	Na^+	K^+	Rb^+	Cs^+
exp polarizability (\AA^3) ^{38,39}	0.15	0.95	1.65	3.08
ab initio polarizability (\AA^3)	0.14	0.79	1.33	2.32
error (%)	7	17	19	25
exp IP (eV)	5.14	4.34	4.18	3.89
ab initio IP (eV)	4.98	4.25	4.08	3.76
error (%)	3	2	2	3

TABLE 2: Polarizability, Vertical Ionization Potential (IP), and Dipole Moment of the Solvent Molecules Both from Experiments and ab Initio MP2 Calculations^a

	water	methanol	dimethyl ether
exp polarizability (\AA^3) ³⁸	1.45	3.25	5.16
ab initio polarizability (\AA^3)	1.25	2.94	4.76
error (%)	14	10	8
ab initio $\Delta\alpha$ (\AA^3)	0.17	0.58	1.01
exp IP (eV)	12.62	10.85	10.03
ab initio IP (eV)	12.69	11.28	10.41
error (%)	1	4	4
exp dipole moment (D)	1.85	1.70	1.30
ab initio dipole moment (D)	1.89	1.71	1.36
error (%)	2	1	5

^a $\Delta\alpha$ is the anisotropy of the polarizability tensor and is defined as $(\Delta\alpha)^2 = 1/2[3\text{Tr}(\tilde{\alpha}^2) - (\text{Tr}\tilde{\alpha})^2]$.

All the ab initio calculations have been performed with GAUSSIAN98.³¹ All the other software are developed in our group.

3. M^+L Model Potential Determination

3.1. Physical Properties of the Cations and Solvents. All the properties have been computed at the ab initio MP2 level of theory and are reported in Table 1 for the cations and Table 2 for the molecules, together with experimental results. We see that the computed properties are generally very close to the experimental ones with the basis sets chosen above and are able to quantitatively reproduce the experimental trends (increase of the polarizability, decrease of the dipole moment, etc.). The polarizabilities are systematically underestimated (max. error: 25%). For the other properties, the maximum error between our calculations and the experimental values does not exceed 5%.

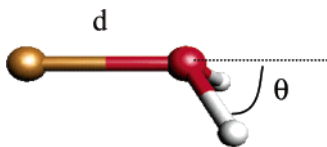
3.2. Ab Initio Results on the M^+H_2O Systems. As in our model potential framework the geometries of the molecules are kept frozen, we have first performed ab initio MP2 calculations on the M^+H_2O systems to evaluate the importance of the geometrical relaxation on the structure and the BSSE-corrected binding energy of the complex. For this purpose, we have first optimized the structure of the complex, the internal geometry of the water molecule being frozen. Then, these constraints have been removed. We have also calculated the ZPE (zero point energy) correction to compare the theoretical binding energies with the experimental ones.

The results thus obtained are summarized in Table 3 and also compared to Glendenning's⁴ ab initio results. The effect of the geometrical relaxation is very small: less than 0.01 \AA on the M^+O equilibrium distance and less than 0.05 kcal/mol on the binding energy. All these results justify the use of a frozen geometry for water in the model potential framework and we assume that this approximation is also valid in the methanol and DME cases. When we compare our binding energies to those of Glendenning, one can see that they are systematically higher; i.e., our dissociation energies are smaller. A possible explanation lies in the larger water dipole moment in Glenden-

TABLE 3: Ab Initio MP2 Results for the $M^+-(H_2O)$ Systems^a

	calculation A			calculation B			calculation C			exp ^b
	R_{O-M}	E_{int}		R_{O-M}	E_{int}	ΔH^{298}	R_{O-M}	E_{int}	ΔH^{298}	
Na ⁺	2.261	22.43		2.265	22.47	-21.80	2.25	24.2	-23.5	-24.0
K ⁺	2.626	16.90		2.625	16.91	-16.38	2.65	18.8	-18.2	-17.9
Rb ⁺	2.795	15.10		2.794	15.14	-14.62	2.90	16.1	-15.5	-15.9
Cs ⁺	3.020	13.06		3.020	13.10	-12.60	3.10	14.0	-13.4	-13.7

^a E_{int} is BSSE-corrected. Distances are given in ångströms and energies in kcal/mol. Calculation A: frozen internal geometry. Calculation B: fully relaxed geometry. Calculation C: Glendening et al.⁴ MP2/6-31+G* calculations. ^b Results of Dzidic et al.³²

**Figure 1.** Description of the structures chosen to obtain the atomic dispersion and repulsion parameters.

ing's calculations: the basis set used (6-31+G*) gives at the MP2 level a water dipole moment of 2.33 D instead 1.89 D in our calculation. When we compare our ZPE-corrected binding energies to the experimental values of Dzidic et al.,³² obtained by mass spectrometry, we can see that our binding energies are higher, whatever the cation. Nevertheless, the decrease of these energies along the series is very satisfactory. We obtain, from Na⁺ to K⁺, 5.5 kcal/mol instead 6.1, from K⁺ to Rb⁺ 1.8 instead 2.0, and from Rb⁺ to Cs⁺, 2.0 instead 2.2. As the relevant properties of the solvent molecules and the cations are well described, and because the variation of our ab initio binding energies is in very good agreement with experimental results, we can have confidence in these ab initio calculations to derive reliable model potential parameters.

3.3. Building the Model Potential: Setting Up Dispersion-Repulsion Parameters for the Alkali Cations. For this purpose, MP2 BSSE-corrected single point binding energy calculations were performed on a large number of M^+-H_2O intermolecular geometries, varying the M^+-O distance between 2.2 and 5 Å (i.e., around the equilibrium value) by steps of 0.1 Å and for five values of the angle θ defined on Figure 1 (0, 30, 50, 70, 90°). This angle has been chosen because the energy variation along this coordinate is very sensitive to possible charge-transfer effects, as already pointed out in the Au^+-H_2O system for example.¹² As the long-range interactions are near-identical between ab initio and model potential calculations, the two atomic parameters needed to express short-range interactions are obtained by the best adjustment of the $E_{int}^{MP2} - (E_{elec} + E_{pol})^{MP}$ values obtained as previously explained. The resulting RRMS (relative root mean squared) error is about 1% for both K⁺ and Rb⁺. The obtained parameter values are $k_{K^+} = 1.86$, $R_{K^+}^w = 1.53$ for K⁺ and $k_{Rb^+} = 2.16$, $R_{Rb^+}^w = 1.63$ for Rb⁺. The structure and binding energy thus obtained are compared with the ab initio ones in Table 4 (in the same table, the previously obtained results¹² on Na⁺ and Cs⁺ are also shown). This comparison shows the capability of our method to reproduce, with only two parameters, the short-range component of the intermolecular interaction. Typical error values are about 0.1 kcal/mol on the binding energy and 0.05 Å on the equilibrium distance. Moreover, the accordance between ab initio and model potential results is good whatever the value of the angle θ . Besides, the long range behavior of the model potential is nearly identical to the ab initio one. Hence, one can be confident in the capacity of the potential to accurately describe the structure

TABLE 4: Comparison between ab Initio MP2 and Model Potential Calculations for the Interaction between an Alkali Cation and a Water Molecule^a

	ab initio MP2		model potential	
	R_{O-M}	E_{int}	R_{O-M}	E_{int}
Na ⁺	2.26	-22.39	2.33	-22.36
K ⁺	2.63	-16.87	2.68	-16.79
Rb ⁺	2.80	-15.10	2.84	-15.05
Cs ⁺	3.01	-13.15	3.02	-13.40

^a Distances are given in ångströms and energies in kcal/mol. The ab initio MP2 E_{int} and distances are BSSE-corrected.

and potential energy of larger clusters if the n-body terms are properly taken into account. Moreover, if the two atomic parameters of both the cations and the oxygen atom are really transferable, no new values of these parameters are needed for the description of $M^+-(CH_3OH)_n$ and $M^+-(DME)_n$ clusters. This last assumption is checked in the next paragraph.

3.4. Transferability of the Atomic Repulsion-Dispersion Parameters. For this purpose, we have performed model potential calculations on the $M^+-(CH_3OH)$ and M^+-DME systems, for all the alkali cations, using the atomic parameters (k_i and R_i^w) already determined. Their transferability is tested, by comparing our model potential results (structures and binding energy) to MP2 BSSE-corrected calculations.

The first problem to be solved is the treatment of the polarization term. In fact, as in the series of solvents, the dipole moment decreases and the electric dipole polarizability increases, the polarization energy is more and more important and any approximation in its calculation should be checked. In this way, we have first tested if we could continue to use the mean electric dipole polarizability (obtained via the additive model of the average bond polarizabilities) to evaluate the polarization energy. The results are not satisfactory in the way that although the binding energies and equilibrium distances of the $M^+-(CH_3OH)$ and M^+-DME systems seem to be correct, many of the obtained structures exhibit a nonzero value for the angle θ (whereas this angle is always equal to zero in ab initio calculations). Moreover, this angle is more important in the DME case whatever the cation is and it decreases from Na⁺ to Cs⁺ (it varies between 40° for Na⁺ and 10° for Cs⁺), so the worst structure is the Na⁺-DME one. Finally, at larger M^+-O distances (~ 5 Å), the equilibrium value of this angle is zero as in the ab initio calculation.

On the other hand, as seen in Table 2, the experimental molecular polarizability greatly increases from water to DME and so does the associated anisotropy. The ratio $\Delta\alpha/\alpha$ (Table 2) represents 17% for water, 20% for methanol, and 22% for DME (obtained by MP2 calculations). Considering the polarizability of water as isotropic is a good approximation: α_{H_2O} is small and the $\Delta\alpha/\alpha$ ratio also; for DME this approximation is less justified, as α_{DME} is more than 3 times larger than α_{H_2O} .

Therefore, to be sure that the discrepancy originates from the use of isotropic bond polarizabilities, we have performed additional calculations on the Na⁺-DME system. For a Na⁺-oxygen distance of 3.5 Å (to prevent any short-range effect), we have calculated the variation with the angle θ of the polarization energy in the isotropic approximation on one hand and the ab initio one on the other hand. The ab initio polarization energy has been obtained at the RHF level by subtracting the first cycle electronic energy to the converged one, the starting guess molecular orbitals being the orthogonalized occupied molecular orbitals of the isolated entities. The two corresponding curves are shown on Figure 2. Clearly, the ab initio polarization

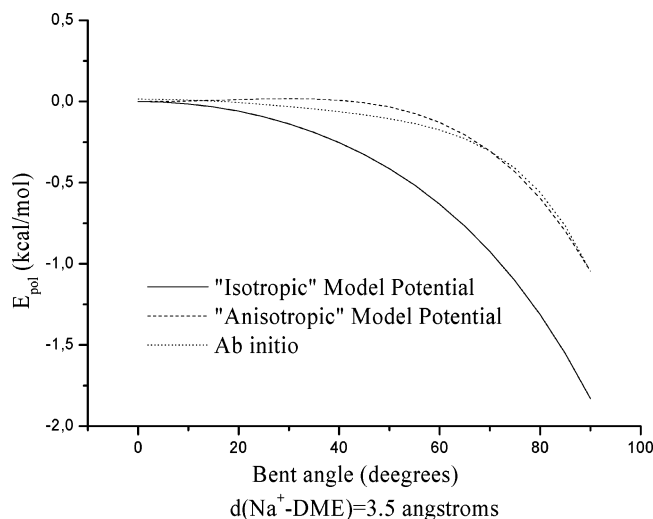


Figure 2. E_{pol} contribution for the Na^+ –DME system, evaluated by ab initio MP2 and model potential methods.

energy increases much more slowly with the angle θ than the isotropic model one. As the electrostatic attractive interaction energy between the cation and the DME molecule decreases as θ increases, also large a variation of the polarization energy can induce a nonzero equilibrium value for this angle. Hence, the isotropic scalar polarizability should be replaced by the overall polarizability tensor of the solvent molecule. Moreover, as previously explained, we have chosen the ratio $\alpha_{kl}^L/\alpha_{kl}^T$ for the O–C and C–H bonds to correctly reproduce the variation of the ab initio polarization energy with θ . The result is also shown on Figure 2. Now, the ab initio and the “anisotropic” curves show the same behavior and are quite parallel. Moreover, if we use these α^L and α^T values in the calculation of the polarizability tensor of the methanol molecule, we obtain a reasonable agreement with the corresponding ab initio tensor. We use the same bond polarizabilities for calculations involving methanol or DME.

With this new approach, the results are the following:

(i) The structures obtained do not exhibit a bent θ angle anymore,

(ii) The “anisotropic” potential energy curve for the Na^+ –DME system reproduces the ab initio one much better than the isotropic does. This is true whatever the cation (see the Rb^+ case on Figure 3),

(iii) As shown in Tables 5 and 6, the variations from Na^+ to Cs^+ (compared to the isotropic model) on the distances and on the binding energies are not very large. However, our new structures are now closer to the ab initio ones so that the average error on the distances is appreciably reduced and the absolute error on the binding energy decreases from about 0.8 to 0.2 kcal/mol in the case of DME. For methanol, the difference between the isotropic and anisotropic case is low and of the same order as the model precision.

The anisotropic scheme has also been applied to the M^+ –(H_2O) systems to check whether modifications are induced. The result of these tests is positive because our previous results are not modified by the use of an anisotropic model. We conclude that our atomic parameters (k_i and R_i^w) are transferable from one system to another, under the condition that other features of the potential terms are properly taken into account, such as the anisotropy of the electric dipole polarizability.

3.5. Cation–One Molecule of Solvent: the Different Terms of the Interaction Energy. In a model potential calculation, it is easy to determine separately all the components

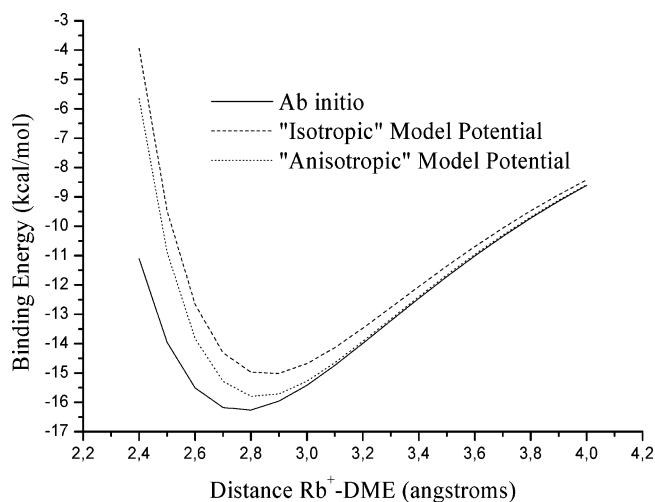


Figure 3. Binding energy of the Rb^+ –DME system evaluated by ab initio and model potential methods.

TABLE 5: Comparison between “Isotropic” and “Anisotropic” Model Potential Binding Energies, for the Interaction between an Alkali Cation and a Molecule of Methanol^a

	ab initio MP2		isotropic model		anisotropic model	
	$R_{\text{O-M}}$	E_{int}	$R_{\text{O-M}}$	E_{int}	$R_{\text{O-M}}$	E_{int}
Na^+	2.26	−23.90	2.32	−23.51	2.30	−24.83
K^+	2.63	−17.94	2.68	−17.59	2.65	−18.35
Rb^+	2.79	−16.09	2.83	−15.73	2.81	−16.35
Cs^+	3.01	−13.95	3.02	−13.99	2.99	−14.59

^a Distances are given in ångströms and energies in kcal/mol.

TABLE 6: Comparison between “Isotropic” and “Anisotropic” Model Potential Binding Energies, for the Interaction between an Alkali Cation and a Molecule of DME^a

	ab initio MP2		isotropic model		anisotropic model	
	$R_{\text{O-M}}$	E_{int}	$R_{\text{O-M}}$	E_{int}	$R_{\text{O-M}}$	E_{int}
Na^+	2.25	−24.09	2.31	−23.57	2.31	−24.44
K^+	2.61	−18.12	2.68	−17.15	2.67	−17.96
Rb^+	2.77	−16.28	2.84	−15.22	2.82	−15.96
Cs^+	2.98	−14.16	3.03	−13.47	3.00	−14.21

^a Distances are given in ångströms and energies in kcal/mol.

of the interaction energy and to study their evolution in a series. Thus, one can display some trends. As seen in Table 7, whatever the solvent, E_{int} decreases from Na^+ to Cs^+ with a gap between Na^+ and the other cations: clearly, the most relevant property is the ionic radius of the cation. Concerning the solvent molecules, the differences are smaller because two opposite effects (dipole vs polarizability) compensate in the total binding energy. Nevertheless, the stability order does not depend on the cation and is methanol \sim DME $>$ water. It should be noticed that, in our ab initio calculation, we found the same order.

As expected, the electrostatic interaction is the smallest in the cation–DME system whereas the opposite situation is observed for the polarization energy. Moreover, although Cs^+ is the cation exhibiting the greatest polarizability, the total polarization energy is always the highest with Na^+ for a given solvent molecule. The ratio $E_{\text{elec}}/E_{\text{pol}}$ varies much in these systems; it is the highest for Cs^+ –water (4.3) and the lowest for Na^+ –DME (1.7). So, in these systems, it seems hazardous to build any model potential without an explicit treatment of the polarization energy. Finally, the dispersion energy component is always very small.

TABLE 7: Analysis of the M^+L Interactions^a

	water					methanol					dimethyl ether				
	E_{elec}	E_{pol}	E_{disp}	E_{rep}	E_{int}	E_{elec}	E_{pol}	E_{disp}	E_{rep}	E_{int}	E_{elec}	E_{pol}	E_{disp}	E_{rep}	E_{int}
Na^+	-21.51	-6.82	-0.84	6.81	-22.36	-21.82	-10.23	-0.95	8.17	-24.83	-19.92	-11.55	-1.04	8.07	-24.44
K^+	-16.54	-4.27	-0.88	4.90	-16.79	-16.65	-6.47	-1.02	5.79	-18.35	-15.04	-7.62	-1.15	5.85	-17.96
Rb^+	-14.88	-3.59	-0.91	4.33	-15.05	-14.92	-5.44	-1.08	5.09	-16.35	-13.41	-6.50	-1.23	5.18	-15.96
Cs^+	-13.18	-3.02	-1.02	3.82	-13.40	-13.27	-4.66	-1.20	4.54	-14.59	-11.87	-5.59	-1.39	4.64	-14.21

^a All values are in kcal/mol. E_{disp} is tabulated $E_{disp} + E_{disp-exch}$.

TABLE 8: Enthalpies from Model Potentials Calculations and Experiments for the Gas-Phase Reactions $M^+ + n[H_2O] \rightarrow M^+ \cdot [H_2O]_n$ in kcal/mol^a

	Na^+		K^+		Rb^+		Cs^+	
	$E - RT$	ΔH^{298}	$E - RT$	ΔH^{298}	$E - RT$	ΔH^{298}	$E - RT$	ΔH^{298}
$M^+ \cdot (H_2O)$	-23.0	-24.0	-17.4	-17.9	-15.7	-15.9	-14.0	-13.7
$M^+ \cdot (H_2O) \cdot (H_2O)$	-20.5	-19.8	-15.5	-16.1	-13.9	-13.6	-12.5	-12.5
$M^+ \cdot (H_2O)_2 \cdot (H_2O)$	-17.1	-15.8	-14.0	-13.2	-14.0	-12.2	-14.0	-11.2
$M^+ \cdot (H_2O)_3 \cdot (H_2O)$	-14.4	-13.8	-13.1	-11.8	-11.7	-11.2	-11.2	-10.6

^a The experimental values are taken from ref 32.

4. Study of $M^+ \cdot (H_2O)_n$, $M^+ \cdot (CH_3OH)_n$, and $M^+ \cdot (O(CH_3)_2)_n$ Systems: Results and Discussion

In the previous section, we have checked the transferability of our atomic parameters from the $M^+ \cdot H_2O$ systems to the $M^+ \cdot CH_3OH$ and $M^+ \cdot DME$ ones. Before using these atomic parameters to study the structure of the first solvation shell and/or perform molecular dynamics calculations, it is important to check if our model potentials, derived from ab initio calculations on “dimers”, are reliable to describe both the structure and the binding energy of larger clusters. In the following we will focus our attention on the $M^+ \cdot L_n$ ($n = 2-4$) clusters and systematically compare our model potential results with ab initio calculations of the literature. We have limited this study to four molecules of solvent surrounding the cation, first because the published ab initio works rarely exceed this number of molecule, and second because for such sizes, our exploration of the PES is nearly exhaustive and ensures that all the lowest minima and particularly the global minimum are found in the model potential calculation.

4.1. General Remarks. The ab initio calculations we will refer to in this section are the following ones: those of Feller and Glendening for $M^+ \cdot H_2O^{4-6}$ and $M^+ \cdot DME^7$ clusters and those of Cabaleiro-Lago et al.^{8,9} for $M^+ \cdot CH_3OH$ clusters. All ab initio calculations performed on these systems used the Hay and Wadt’s ECP for K^+ , Rb^+ , and Cs^+ and the associated valence basis set;³³ they have been augmented with d-type polarization functions, whose exponents are $\alpha_d(K) = 0.48$, $\alpha_d(Rb) = 0.24$, and $\alpha_d(Cs) = 0.19$.⁴ The use of these ECP and basis sets results in an underestimation of the cations polarizabilities (they are respectively 0.59, 1.07, and 1.79 Å³ for K^+ , Rb^+ , and Cs^+). It is important at this stage to recall the underlying assumptions before comparing ab initio results of the literature and our model potential ones:

(i) In our model potential, the n-body terms other than the polarization are neglected.

(ii) The cation polarizabilities we used in our model potential calculations are the experimental ones, which are noticeably larger than the ab initio ones (see above). This fact can explain most of the structural differences we observe (see below).

(iii) Unfortunately, the ab initio binding energies are not always BSSE-corrected. Moreover, the results of the literature do not always provide both binding energies and structural data.

(iv) Some local minima, nearly isoenergetic with the global one in our model potential calculations but with a very different structure, have not been studied by ab initio methods.

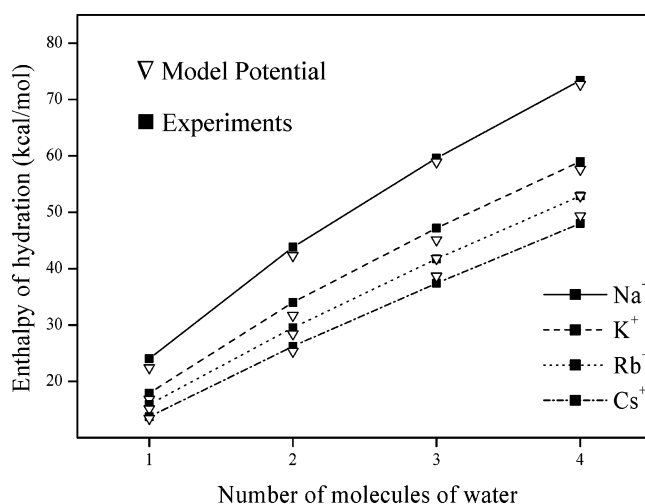


Figure 4. Comparison of the enthalpies of hydration (kcal mol⁻¹) obtained from model potential calculations and experiments.³²

Three main criteria were used in the following for a careful comparison of our results with experimental and/or theoretical data. The first is the binding energy and its variation with the number of solvent molecules. The second criterion is based on the comparison of the geometrical structures. We focus especially on the variation of the M–O distance with the size of the cluster and on some O–cation–O angles. The third corresponds to some “filament” structures containing m molecules in the first coordination sphere and one in the second, which often exhibit binding energies very similar to those of a compact structure with $(m + 1)$ molecules in the first coordination sphere.

4.2. Binding Energies. If we compare the evolution of the total binding energies corresponding to the global minimum with the size of the clusters, obtained with model potential calculation, with the experimental enthalpies of hydration of Dzidic and Kebarle,³² one can see that these evolutions are very similar whatever the cation (Figure 4). One can also compare the variation with the size of the successive binding energies for an extra water molecule (Table 8). The decrease of the binding energy with the size is well reproduced and the agreement with experimental results is independent of this size.

We have performed the same work on the $M^+ \cdot (DME)_n$ systems and will compare our binding energies to experimental ones. In Table 9 are summarized our calculated energies together with the experimental ones of Armentrout et al.³⁴ These results

TABLE 9: Binding Energies E from Model Potential Calculations and Experiments for the Gas-Phase Reactions $M^+-(DME)_{n-1} + DME \rightarrow M^+-(DME)_n$ in kcal/mol^a

	Na ⁺		K ⁺		Rb ⁺		Cs ⁺	
	E	ΔH^0	E	ΔH^0	E	ΔH^0	E	ΔH^0
$M^+-(DME)$	-24.4	-21.9	-18.0	-17.5	-15.9	-14.8	-14.2	-13.6
$M^+(DME)-DME$	-20.9	-19.6	-15.6	-16.4	-14.2	-13.1	-13.0	-11.3
$M^+(DME)_2-DME$	-17.1	-16.6	-13.8	-13.6	-12.8	-8.8	-12.1	-9.5
$M^+(DME)_3-DME$	-14.5	-14.5	-11.8	-12.0	-10.8	-9.2	-10.0	-8.5

^a The experimental values are taken from ref 34 and references therein. Values in italics indicate estimated values.

TABLE 10: $\Delta l_{n \rightarrow n+1}$, the Lengthening of the Mean Na⁺–O Distance (Å) between Na⁺–(H₂O)_n and Na⁺–(H₂O)_{n+1}

	model potential	ab initio MP2
$\Delta l_{1 \rightarrow 2}$	0.029	0.012
$\Delta l_{2 \rightarrow 3}$	0.035	0.033
$\Delta l_{3 \rightarrow 4}$	0.028	0.024

have been obtained by means of collision-induced dissociation. The agreement is as good as for water clusters, except for $n = 3, 4$ with Rb⁺ and Cs⁺. However, the Rb⁺–(DME)₄ and Cs⁺–(DME)₄ experimental values are estimated ones. Moreover, according to the authors, these measurements, especially for the higher clusters, could have been done on nonfundamental systems (i.e., presence of less strongly bound conformers that are formed by kinetically favored processes in the experimental ion source). The main result of this comparison is that we obtain in model potential calculations the same accuracy for both the small and the large clusters.

We also compare our results with some ab initio results for compact structures. The general trend of the decreasing binding energy is almost the same, in view of the expected accuracy of both ab initio and model potential methods. The absolute error does not exceed 1 kcal/mol and is often smaller. Same conclusions can be obtained for the other cations for both water and DME clusters. We can conclude that neglecting the n -body contributions other than the polarization one is a good approximation.

4.3. Geometrical Structures. We now focus on the structures obtained by ab initio and model potential calculations.

The first point to discuss is the modification of the metal–oxygen distance with the size of the cluster in the compact clusters. For the smallest sizes, i.e., when the first solvation shell is not “full”, the interaction of the solvent molecules with the newly added molecule is repulsive because their dipole moments (permanent as well as induced) exhibit a mutual orientation leading to a repulsive electrostatic interaction. For this reason, the metal–oxygen distance necessarily increases and the mean binding energy decreases, as quoted in the previous paragraph. It is thus interesting to compare the ab initio increase of this cation–oxygen distance with the model potential one. As this comparison is especially meaningful for $(n + 0)$ structures, we have chosen unambiguous situations, for example, the water clusters up to $n = 4$ with Na⁺ (Table 10). The increment of the M–O distance obtained with our model potential is slightly larger in the $2 \rightarrow 3$ and $3 \rightarrow 4$ cases, too large by 0.017 Å in the $1 \rightarrow 2$ case. The results are also very satisfying in the methanol and DME case (increment of 0.1 Å from 1 to 4 solvent molecules).

We will discuss now the spatial layout of the solvent molecules around the cation. To simplify the following discussion, we only consider the positions of the oxygen atoms. The most stable minima observed are shown in Figures 5–7.

In these systems bound mainly by electrostatic forces, this

TABLE 11: $M^+-(DME)_2$ Optimized Structures

	model potential	ab initio MP2
Na ⁺ (DME) ₂	179.1	180.0
K ⁺ (DME) ₂	88.7	88.8
Rb ⁺ (DME) ₂	82.2	81.1
Cs ⁺ (DME) ₂	76.1	74.9

^a Structural data for the O–M⁺–O angle (deg) results of Hill et al.⁷ MP2/6-31+G* optimized structures.

TABLE 12: Comparison between C_{4v} and T_d Binding Energies in the $M^+-(H_2O)_4$ Case^a

	Na ⁺		K ⁺		Rb ⁺		Cs ⁺	
	C_{4v}	T_d	C_{4v}	T_d	C_{4v}	T_d	C_{4v}	T_d
MP	no	yes	0.	−0.3	0.	1.5	0.	4.
ab initio/MP2	no	yes	0.	−0.5	0.	2.3	0.	4.6

^a The binding energy of the C_{4v} structure is taken equal to zero. Energies are given in kcal/mol.

spatial layout is the result of the competition between two antagonistic effects: on one hand, the repulsive interaction between solvent molecules has to be minimized, leading to highly symmetrical structures: D_h for two molecules, D_{3h} for three, T_d for four. On the other hand, maximizing the polarization energy of the cation leads to structures of lower symmetry, because the electric field created on the cation by the solvent molecules will exhibit a nonzero value: we thus obtain C_{2v} structure for $n = 2$, C_{3v} for $n = 3$, and C_{4v} for $n = 4$. From this discussion, it is easy to understand that (i) the potential energy surface can be very flat along this deformation coordinate and (ii) the obtained structure greatly depends on the polarizability of the cation.

The first effect is predominant for weakly polarizable cations such as Na⁺. It is strictly the opposite situation for a very polarizable cation such as Cs⁺. A more quantitative comparison is shown in Table 11 concerning the O–M⁺–O angle in $M^+-(DME)_2$ clusters. The agreement between ab initio results of Hill et al. and our model potential results is very good. Another interesting example is the $M^+(H_2O)_4$ case. The energetic difference between T_d and C_{4v} structures in the series of cations is shown in Table 12. This difference is described in a quantitative way by model potential calculations (in the case of Na⁺, neither ab initio calculation nor model potential give any stable C_{4v} structure).

4.4. “Filament” Structures. As water and methanol can form strong hydrogen bonds, one can obtain structures where one solvent molecule is not directly bound to the cation (“filament” structure). In this section, we will only consider the competition $(2 + 1)$ vs $(3 + 0)$ and $(3 + 1)$ vs $(4 + 0)$ in the case of water.

For the $M^+-(H_2O)_3$ case, the main point is the existence, for all the cations, in model potential as well as in ab initio calculations, of two local minima corresponding to the two structures. The energetic order is not as good. For example, though the agreement is quite perfect in the case of Na⁺ (the $(3 + 0)$ is the most stable with a difference of 3 kcal/mol in our calculation and of 2.9 kcal/mol in ab initio results),⁴ some discrepancies are found in some other cases. Another example is the case of K⁺–(H₂O)₃ for which the $(2 + 1)$ and the $(3 + 0)$ structures exhibit very similar binding energies, whereas Glendening et al. found the $(3 + 0)$ to be the most stable by 1.1 kcal/mol. For Rb⁺, the two structures have the same binding energy in ab initio calculations but are separated by 1.5 kcal/mol in the model potential method, the $(2 + 1)$ being most stable. Analogous remarks can be made in the $M^+-(H_2O)_4$ case. Similarly, for $n = 3$, the two structures are local minima in the

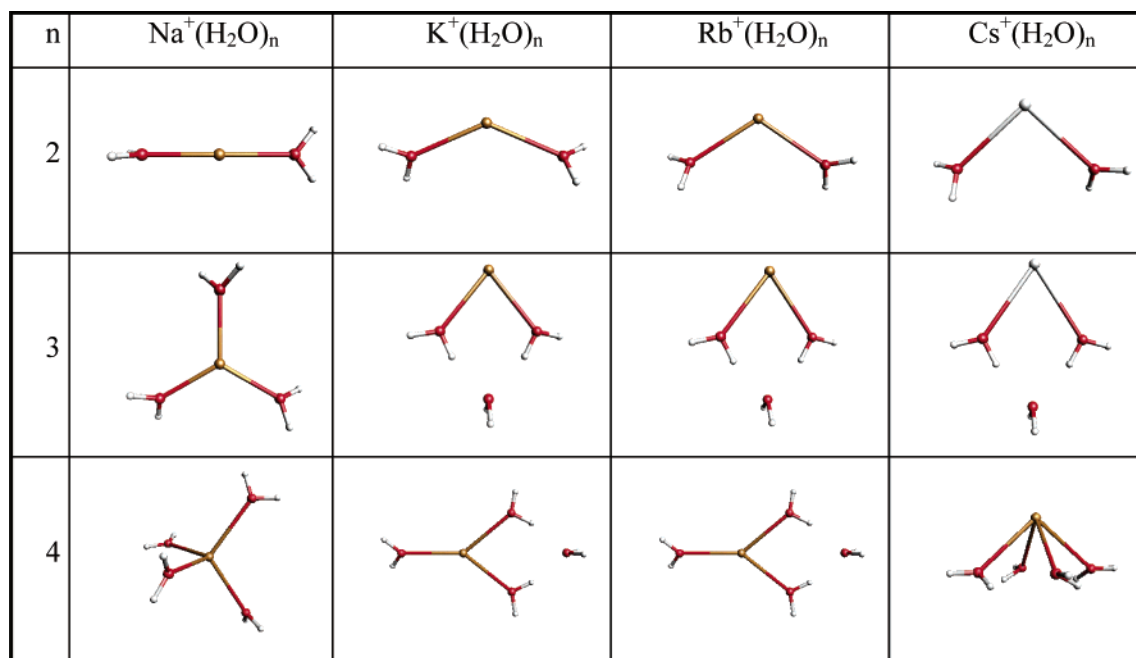


Figure 5. Most stable minima obtained with the MCGM for $\text{M}^+(\text{H}_2\text{O})_{n=2-4}$.

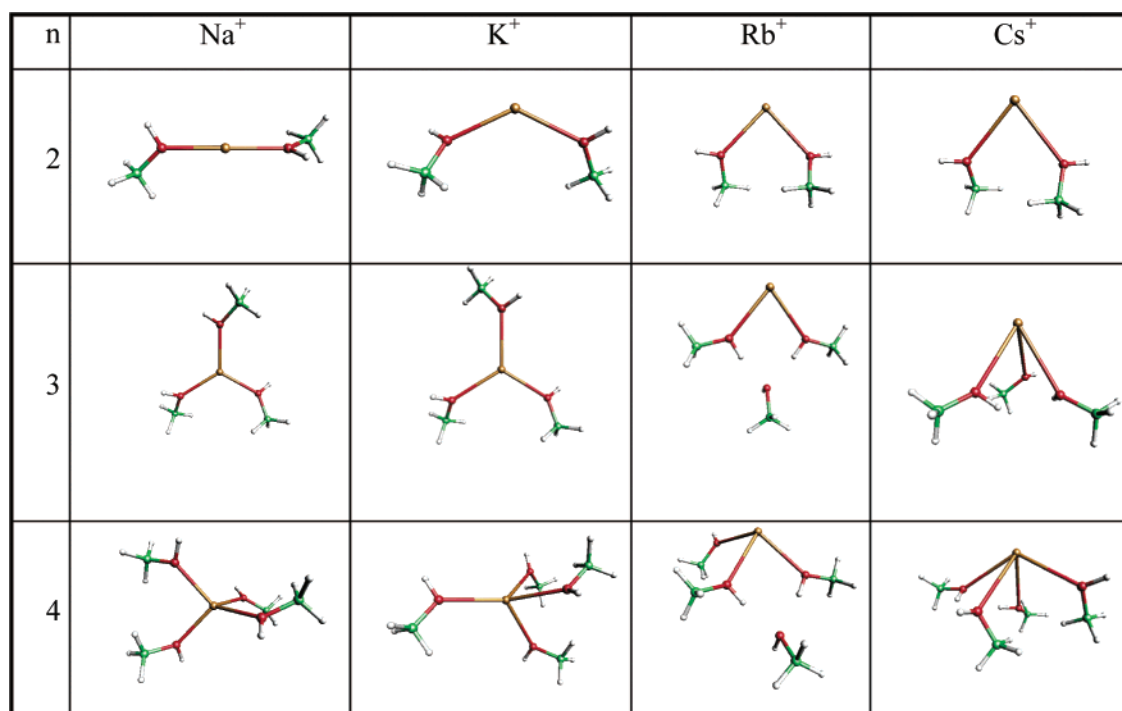


Figure 6. Most stable minima obtained with the MCGM for $\text{M}^+(\text{CH}_3\text{OH})_{n=2-4}$.

two methods, but the stability order is not always the same. However, a general trend appears: the model potential gives an advantage to “filament” structures. This fact is very probably due to the difference between the model potential and HF + MP2 method in the description of the hydrogen bond.

5. Summary, Conclusions, and Perspectives

The building of a model potential, including polarization energy as an n -body term, for the interaction between alkali cations (from Na^+ to Cs^+) and three different solvent molecules (water, methanol and DME), has been described. A precision comparable to that of ab initio results can be obtained by taking into account the anisotropy of the electric dipole polarizability

tensor for the solvent. This anisotropy can be described by using a simple model of longitudinal and transverse chemical bond polarizabilities. Moreover, the “atomic” parameters used in the parametrization of the short-range interactions are found to be transferable, for the alkali cations as well as for the oxygen atom of the three solvent species.

The adequacy of this model potential to describe energetic and structural properties of small $\text{M}^+(\text{solvent})_n$ ($n = 2-4$) clusters has been shown by comparison with experimental and ab initio results. The decrease of the mean binding energy and the lengthening of the $\text{M}-\text{O}$ distance when the size of the cluster increases are very well reproduced. The competition between the minimization of the repulsive interaction between solvent

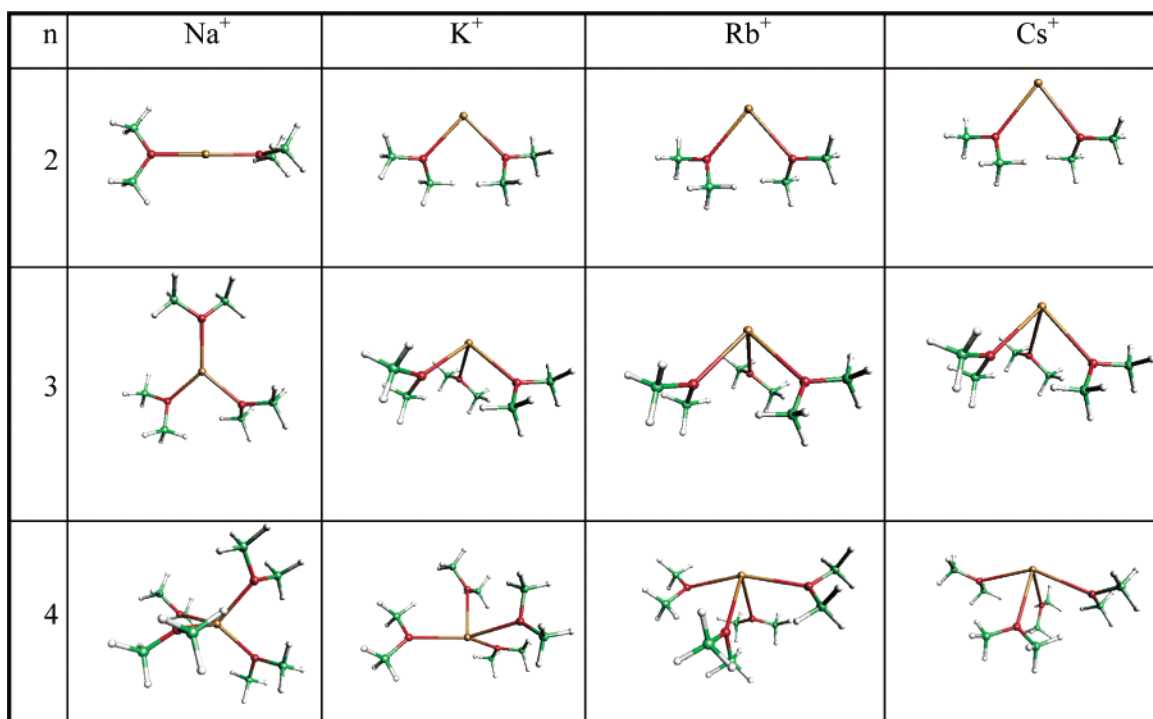


Figure 7. Most stable minima obtained with the MCGM for $M^+(O(CH_3)_2)_n$, $n=2-4$.

molecules and the maximization of the polarization energy of the cation is also well described. All these results show unambiguously that the only important many-body term for the description of such systems is the polarization one. In conclusion, one can expect to obtain, in liquid-phase molecular dynamics calculations, an accuracy analogous to that one can expect to obtain by using ab initio methods, but at shorter simulation times. Work on the structure of the first solvation shell in all these systems as well as the study of mixed clusters is in progress.

6. Appendix

The general formula for the evaluation of the total polarization energy is³⁵

$$E_{\text{pol}} = -\frac{1}{2} \sum_i \vec{E}_i \vec{\alpha}_i \vec{E}_i^0$$

where the sum includes all the polarizable sites with a polarizability tensor $\vec{\alpha}_i$. \vec{E}_i^0 is the electric field created on the site i by permanent multipolar multicentric distribution, \vec{E}_i is the total electric field and can be expressed as

$$\vec{E}_i = \vec{E}_i^0 + \sum_j \vec{T}_{ij} \vec{\mu}_j$$

With $\vec{\mu}_j = \vec{\alpha}_j \vec{E}_j$ and \vec{T}_{ij} defined as

$$(\vec{T}_{ij})_{kl} = \left(\frac{1}{\vec{r}_{ij}^3} \left[3 \frac{\vec{r}_{ij}^k \vec{r}_{ij}^l}{r_{ij}^2} - \delta_{kl} \right] \right)$$

In our model potential framework, the sites are the atoms and the “electronic barycenter” of each bond. The determination of the polarizability tensors $\vec{\alpha}$ on each site is the following. We start from the theory of Lefevre. With each bond kl is associated a polarizability tensor $\vec{\alpha}_{kl}$ that is diagonal in the local frame associated with the bond (one axis is parallel to this bond; the two others are perpendicular). These tensors can be written α_{kl}^L ,

α_{kl}^T , and α_{kl}^T (L = longitudinal, T = transverse). The mean bond polarizability is expressed as $\bar{\alpha}_{kl} = 1/3(\alpha_{kl}^L + 2\alpha_{kl}^T)$ and the total molecular polarizability as

$$\alpha_M = \sum_{kl \in M} \bar{\alpha}_{kl}$$

This bond polarizability tensor $\vec{\alpha}_{kl}$ is split among the two atoms k and l and the “electronic barycenter” G_{kl} of the bond kl according to the following procedure:^{36,37}

$$\vec{\alpha}_{Gkl} = \vec{\alpha}_{kl} \frac{\left(\frac{n_{kl}}{2} \right)}{\left(n_{kl} + \frac{n_k}{N_k} + \frac{n_l}{N_l} \right)}$$

where (i) n_{kl} is the number of electrons in the bond kl (2 for a single bond, 4 for a double bond, etc.), (ii) n_k and n_l are the number of lone pair valence electrons located on the atoms k and l , respectively, and (iii) N_k and N_l are the number of bonds starting from the atoms k and l , respectively.

On the atom k (respectively l) the contribution of the bond kl is calculated as

$$\vec{\alpha}_{k(kl)} = \vec{\alpha}_{kl} \frac{\left(\frac{n_{kl}}{4} + \frac{n_k}{N_k} \right)}{\left(n_{kl} + \frac{n_k}{N_k} + \frac{n_l}{N_l} \right)}$$

It is easy to verify that this procedure does not modify the mean molecular polarizability.

References and Notes

- Izatt, R. M.; Pawlak, K.; Bradshaw, J. S. *Chem. Rev.* **1991**, *91*, 1721.
- Solov'ev, V. P.; Strakhova, N. N.; Raevsky, O. A.; Rüdiger, V.; Schneider, H.-J. *J. Org. Chem.* **1996**, *61*, 5221.

- (3) Islam, M. S.; Pethrick, R. A.; Pugh, D.; Wilson, M. J. *J. Chem. Soc., Faraday Trans.* **1998**, 94, 39.
- (4) Glendening, E. D.; Feller, D. *J. Phys. Chem.* **1995**, 99, 3060.
- (5) Feller, D.; Glendening, E. D.; Woon, D. E.; Feyereisen, M. W. *J. Chem. Phys.* **1995**, 103, 3526.
- (6) Feller, D. *J. Phys. Chem. A* **1997**, 101, 2723.
- (7) Hill, S. E.; Glendening, E. D.; Feller, D. *J. Phys. Chem. A* **1997**, 101, 6125.
- (8) Garcia-Muruais, A.; Cabaleiro-Lago, E. M.; Hermida-Ramon, J. M.; Rios, M. A. *Chem. Phys.* **2000**, 254, 109.
- (9) Cabaleiro-Lago, E. M.; Rodriguez-Otero, J. *J. Phys. Chem. A* **2002**, 106, 7195.
- (10) Kim, J.; Lee, S.; Cho, S. J.; Mhin, B. J.; Kim, K. S. *J. Chem. Phys.* **1995**, 102, 839.
- (11) Marcus, Y. *Ion Solvation*; Wiley: New York, 1985.
- (12) Derepas, A.-L.; Soudan, J.-M.; Brenner, V.; Dognon, J.-P.; Millié, P. *J. Comput. Chem.* **2002**, 23, 1013.
- (13) Lefevre, R. J. W. In *Advances in Physical Organics Chemistry*; Academic Press: New York, 1965; Vol. 3, p 1.
- (14) Kitagorodskii, A. I. *Tetrahedron* **1961**, 14, 975.
- (15) Garel, T.; Orland, H. *J. Phys. A* **1990**, 23, L621.
- (16) Garel, T.; Niel, J. C.; Orland, H.; Velikon, B. *J. Chim. Phys.* **1991**, 88, 2473.
- (17) Poteau, R.; Spiegelman, F. *J. Chem. Phys.* **1993**, 98, 6540.
- (18) Poteau, R.; Spiegelman, F. *J. Chem. Phys.* **1993**, 99, 10089.
- (19) Bertolus, M.; Brenner, V.; Millié, P.; Maillet, J.-B. *Z. Phys. D* **1997**, 39, 239.
- (20) Gregoire, G.; Brenner, V.; Millié, P. *J. Phys. Chem. A* **2000**, 104, 5204.
- (21) Fletcher, R. *Comput. J.* **1970**, 13, 317.
- (22) Goldfarb, D. *Math. Comput.* **1970**, 24, 23.
- (23) Shanno, D. F. *Math. Comput.* **1970**, 24, 647.
- (24) van Duijneveldt, F. B. *IBM Res. Rep.* **1971**, RJ945.
- (25) Pacios, L. F.; Christiansen, P. A. *J. Chem. Phys.* **1985**, 82, 2664.
- (26) Hurley, M. M.; Pacios, L. F.; Christiansen, P. A.; Ross, R. B.; Ermler, C. *J. Chem. Phys.* **1986**, 84, 6840.
- (27) Lajohn, L. A.; Christiansen, P. A.; Ross, R. B.; Atashroo, T.; Ermler, C. *J. Chem. Phys.* **1987**, 87, 2812.
- (28) Ross, R. B.; Powers, J. M.; Atashroo, T.; Ermler, C.; Lajohn, L. A.; Christiansen, P. A. *J. Chem. Phys.* **1990**, 93, 6654.
- (29) Hoyau, S.; Ohanessian, G. *Chem. Eur. J.* **1998**, 4, 1561.
- (30) Boys, S. F.; Bernardi, F. *Mol. Phys.* **1970**, 19, 553.
- (31) Frisch, M. J.; Trucks, G. W.; Schlegel, H. B.; Scuseria, G. E.; Robb, M. A.; Cheeseman, J. R.; Zakrzewski, V. G.; Montgomery, J. A.; Stratmann, R. E.; Burant, J. C.; Dapprich, S.; Millam, J. M.; Daniles, A. D.; Kudin, K. N.; Strain, M. C.; Farkas, O.; Tomasi, J.; Barone, V.; Cossi, M.; Cammi, R.; Mennucci, B.; Pomelli, C.; Adamo, C.; Clifford, S.; Ochterski, J.; Petersson, G. A.; Ayala, P. Y.; Cui, Q.; Morokuma, K.; Malick, D. K.; Rabuck, A. D.; Raghavachari, K.; Foresman, J. B.; Cioslowski, J.; Ortiz, J. V.; Stefanov, B. B.; Liu, G.; Liashenko, A.; Piskorz, P.; Komaromi, I.; Gomperts, R.; Martin, R. L.; Fox, D. J.; Keith, T.; Al-Laham, M. A.; Peng, C. Y.; Nanayakkara, A.; Gonzalez, C.; Challacombe, M.; Gill, P. M. W.; Johnson, B. G.; Chen, W.; Wong, M. W.; Andres, J. L.; Head-Gordon, M.; Replogle, E. S.; Pople, J. A. *Gaussian 98*, revision A7 ed.; Gaussian, Inc.: Pittsburgh, PA, 1998.
- (32) Dzidic, I.; Kebarle, P. *J. Phys. Chem.* **1970**, 74, 1466.
- (33) Hay, P. J.; Wadt, W. R. *J. Chem. Phys.* **1985**, 82, 299.
- (34) Armentrout, P. B. *Int. J. Mass Spectrom.* **1999**, 193, 227.
- (35) Ahlström, P.; Wallqvist, A.; Engström, S.; Jönsson, B. *Mol. Phys.* **1989**, 68, 563.
- (36) Caillet, J.; Claverie, P. *Acta Crystallogr.* **1975**, A31, 448.
- (37) Gresh, N.; Claverie, P.; Pullman, A. *Int. J. Quantum Chem., Quantum Chem. Symp.* **1979**, 13, 243.
- (38) *Handbook of Chemistry and Physics*; CRC Press: Boca Raton, FL, 1996.
- (39) Fraga, S.; Karwowski, J.; Saxena, K. M. S. *Handbook of Atomic Data*; Elsevier: Amsterdam, 1976.